



Original software publication

MicroFEA 1.0 – A software package for Finite Element Analysis of functionally graded materials



Marcelo S. Medeiros Jr. *, Evandro Parente Jr.

Laboratório de Mecânica Computacional e Visualização, Departamento de Engenharia Estrutural e Construção Civil, Universidade Federal do Ceará, Fortaleza, Brazil

ARTICLE INFO

Article history:

Received 19 July 2019

Received in revised form 9 April 2020

Accepted 9 April 2020

Keywords:

FGM

Finite Element Analysis

Micromechanics

UMAT

ABSTRACT

Functionally Graded Materials (FGM) are a class of advanced composites with a gradual and continuously varying microstructural composition. This paper presents MicroFEA 1.0, which is a software package developed to help overcoming the challenges of designing and analyzing FGM structures. It provides capabilities to fit FGM experimental data to B-Spline curves and to analyze composite materials using mean-field micromechanics homogenization techniques. The package is composed of MATLAB scripts and Fortran subroutines intended for Finite Element Analysis (FEA) using Abaqus. The Abaqus user-material subroutines (UMATs) are designed to work with heterogeneous materials at the integration points level, discarding the need for custom-designed elements. Thermomechanical analyses can also be carried out with the help of UTEMPs. This software will provide valuable help for scientists and engineers facing the development of new FGM structural components.

© 2020 The Authors. Published by Elsevier B.V. This is an open access article under the CC BY license (<http://creativecommons.org/licenses/by/4.0/>).

Code metadata

Current code version	v1.0
Permanent link to code/repository used for this code version	https://github.com/ElsevierSoftwareX/SOFTX_2019_244
Legal Code License	GNU General Public License
Code versioning system used	none
Software code languages, tools, and services used	MATLAB, Fortran
Compilation requirements, operating environments & dependencies	Fortran Intel Compiler ver. 11.1 or above
If available Link to developer documentation/manual	N/A
Support email for questions	marcelomedeiros@ufc.br

1. Motivation and significance

The demand for a high-performance thermal barrier that could withstand the elevated temperatures from space vehicles reentries and fusion reactors originated a new class of composites called Functionally Graded Materials (FGMs) [1–3]. Functionally graded materials are a family of advanced composites formed by two or more constituent phases (matrix and inclusions) with a gradual and continuously varying microstructural composition. This facilitates the development of high-performance structural components with different functional characteristics within different sections of the same part.

The changes in material properties can be engineered to reduce in-plane and out-of-plane stresses, prevent delamination, alleviate residual stresses and improve wear resistance. FGMs have also improved thermal, electric and magnetic attributes when compared to those of the homogeneous counterparts [4–7]. FGM composites find applications in aerospace [8], nuclear [9], automotive [10] and biomedical [11] industries, to name a few. Nonetheless, the technologies to produce FGM composites have not reached their maturity yet and are expected to have a growing impact on the design and development of new components and structures in the near future.

Some studies on Finite Element Analysis of FGM were carried out based on custom-made subroutines for Abaqus [12–16], but none of the codes were made available by the authors. That makes it difficult to replicate and improve upon the reported results.

* Corresponding author.

E-mail addresses: marcelomedeiros@ufc.br (M.S. Medeiros Jr.), evandro@ufc.br (E. Parente Jr.).

Moreover, no major commercial finite element software has the built-in capabilities to address the spatial variation of thermal and/or mechanical properties throughout the geometry of the structure using micromechanics homogenization. It is therefore paramount to pursue the necessary means to predict the response of FGM elements subjected to thermal and mechanical loads.

This paper presents the MicroFEA 1.0 package for finite element analysis of functionally graded materials. The software package is aimed at providing a suite of tools capable of fulfilling the scientific and industrial needs for simulation of the behavior of advanced structural FGM components, specially under complex thermomechanical fields.

The volume fraction profile can be represented either by conventional closed-form mathematical expressions (e.g. power-law, exponential, and sigmoidal) or B-Splines. The former approach is widely used in the analysis and design of functionally graded structures due its simplicity, while the latter gives more flexibility to design optimization [17] and allows for a more accurate representation of the actual volume fraction variation measured in the laboratory.

For instance, MicroFEA 1.0 has been recently used to investigate the effects of the different homogenization schemes on the mechanical behavior of pressurized Al/SiC FGM cylinders [18]. The use of B-Splines to account for the actual volume fraction distribution of tested specimens resulted in significant differences in the hoop and radial stresses when compared to the use of simple closed-form mathematical approximations of the same distribution.

2. Software description

The main characteristic of FGMs is the continuous variation of the volume fraction of its constituents throughout the geometry of the structure. Since the behavior of a composite material depends on the properties of each phase and their relative proportions, the volume fraction variation has a major impact on the thermomechanical performance of FGM structural components. Therefore, the analysis of FGM components involves two important aspects: the definition of the volume fraction in each point of the component and the evaluation of the effective composite properties at each point from the properties and the volume fractions of each phase. These aspects are discussed in the following section.

2.1. Theoretical foundations

Generally, simple mathematical functions (e.g. power-law, exponential, and sigmoidal) are used to describe the volume fraction variation in a FGM part [2]. For instance, the power-law function is commonly used for metal–ceramic FGM plates:

$$V_f = \left(\frac{1}{2} + \frac{z}{h} \right)^N, \quad V_m = 1 - V_f \quad (1)$$

where V_f and V_m are the volume fraction of the ceramic and metal phases, respectively, h is the plate thickness, $z \in [-h/2; h/2]$, and N is the exponent that characterize the material distribution.

This expression is convenient in the design of FGM structures because it requires the definition of only one parameter to describe the volume fraction distribution. However, the literature also shows that the actual distribution of inclusions may not be accurately described by monotonically increasing or decreasing functions. FGM composites formed by centrifugal casting, for instance, have their spatially varying compositional structure determined by the difference in density between reinforcing particles and a molten metal matrix, the applied centrifugal force, the particle size, the viscosity of the melt, the volume fraction

of particles and the solidification time [19,20]. This way, the need for a more flexible family of parametric curves capable of capturing the jaggedness of the actual volume fraction profile curve becomes apparent.

A B-Spline curve $C(\xi)$ is a piece-wise polynomial function of degree p of the parametric coordinate ξ defined as linear combination of the basis functions $N_{i,p}$ and a set of control points \mathbf{p}_i :

$$C(\xi) = \sum_{i=1}^n N_{i,p} \mathbf{p}_i \quad (2)$$

The definition of $N_{i,p}$ basis requires a knot vector, composed by non-negative and non-decreasing parametric values bounded by the parametric interval in which the curve is defined [21]. Given a knot vector $\Xi = [\xi_1, \xi_2, \dots, \xi_{n+p+1}]$, the B-Splines basis functions are calculated by the recursive Cox–de Boor formula [21]:

$$N_{i,0}(\xi) = \begin{cases} 1, & \xi_1 \leq \xi \leq \xi_{i+1} \\ 0, & \text{otherwise} \end{cases} \quad (3a)$$

$$N_{i,p}(\xi) = \frac{\xi - \xi_i}{\xi_{i+p} - \xi_i} N_{i,p-1}(\xi) + \frac{\xi_{i+p+1} - \xi}{\xi_{i+p+1} - \xi_{i+1}} N_{i+1,p-1}(\xi) \quad (3b)$$

The continuity of the basis across the knots are controlled by the knot multiplicity [21].

For any chosen knot vector, the curve shape can be easily controlled by changing the coordinates of the control points (\mathbf{p}_i), which is very useful for interactive manipulation of curve shapes to model complex geometries. Therefore, they are widely used in the CAD systems to model free-form curves and surfaces. In MicroFEA 1.0 the volume fraction variation along the chosen direction can be described as a B-Spline function:

$$V_f(\xi) = \sum_{i=1}^n N_{i,p} V_{f_i} \quad (4)$$

where V_{f_i} are the volume fraction at the control points. Open knot vectors [21] with $\xi_i \in [0, 1]$ are used in the computational implementation. The volume fractions V_{f_i} are computed using the least squares method to fit the B-Spline to the actual volume fraction distribution measured experimentally. The least squares method was chosen due to its simplicity and accuracy. Moreover, B-Splines have been used to represent the volume fraction distribution in FGM optimization using the volume fractions V_{f_i} as design variables [17], since they offer more design flexibility than simple closed-form mathematical functions.

In addition, B-Splines can also be used to represent directly the distribution of material parameters throughout the FGM component. For instance, the Young's modulus variation can be represented as

$$E(\xi) = \sum_{i=1}^n N_{i,p} E_i \quad (5)$$

where E_i are the Young's modulus at the control points. Similar expressions are used for the Poisson's ratio $\nu(\xi)$ and the coefficient of thermal expansion $\alpha(\xi)$.

The mean-field homogenization theory is used to obtain the effective properties of the composite material (E_{hom} and ν_{hom}) at each point of the FGM part. In mathematical terms, a boundary value problem is comprised of a differential equation together with a set of additional constraints, called the boundary conditions. If the function satisfying the boundary condition continues to be valid when multiplied by a scale factor, the boundary is said to be homogeneous [22]. It can also be shown that a homogeneous boundary condition applied on the surface of a statistically homogeneous body (RVE) generates a homogeneous field inside

of it [23]. The homogeneity is defined by postulating that strain and stress averages, for homogeneous boundary conditions, are the same over randomly chosen RVE. Therefore, homogeneous boundary tractions or displacements are imposed on the faces of the RVE, and the average stress or strain fields are used to determine the effective material properties of the composite.

According to this theory, the volume-averaged strains within the inclusion (ϵ_{ij}^{inc}) can be related to the overall strain conditions (ϵ_{kl}) by means of fourth-order concentration tensors A_{ijkl} :

$$\langle \epsilon_{ij}^{inc} \rangle = A_{ijkl} \langle \epsilon_{kl} \rangle \quad (6)$$

The different homogenization schemes will differ by the expression of A_{ijkl} , but in all of them the macro-stiffness tensor of the two-phase composite is written as [24]:

$$C_{ijkl}^{hom} = \left[C_{ijop}^{mat} + V_f (C_{ijmn}^{inc} - C_{ijmn}^{mat}) A_{mnop} \right] \left[V_f A_{opkl} + V_m I_{opkl} \right]^{-1} \quad (7)$$

where I_{opkl} corresponds to the fourth order symmetric unit tensor and V_f and V_m are the volume fraction of the inclusions and matrix respectively. The homogenized modulus and Poisson's ratio are calculated according to the following relations [25]:

$$E_{hom} = \frac{1}{S_{1111}} \quad (8)$$

$$\nu_{hom} = -\frac{S_{1122}}{S_{1111}} \quad (9)$$

where $S_{ijkl} = (C_{ijkl})^{-1}$. After that, the Lamé's constants λ and μ are calculated from the homogenized modulus E_{hom} and Poisson's ratio ν_{hom} :

$$\lambda = \frac{E_{hom} \nu_{hom}}{(1 + \nu_{hom})(1 - 2\nu_{hom})} \quad (10)$$

$$\mu = \frac{E_{hom}}{2(1 + \nu_{hom})} \quad (11)$$

Finally, these constants are used to assemble the elastic constitutive matrix of the homogenized material and calculate the stresses according to

$$\sigma_{ij} = C_{ijkl} (\epsilon_{kl} - \alpha \Delta T \delta_{kl}) \quad (12)$$

where α is the volume fraction-dependent coefficient of thermal expansion which is homogenized according to Turner's model [26]. It is important to note that the actual implementation uses the Voigt notation for 3D analysis and Eq. (12) is coded in the matrix format as

$$\begin{Bmatrix} \sigma_{11} \\ \sigma_{22} \\ \sigma_{33} \\ \sigma_{23} \\ \sigma_{13} \\ \sigma_{12} \end{Bmatrix} = \begin{bmatrix} \beta & \lambda & \lambda & 0 & 0 & 0 \\ \lambda & \beta & \lambda & 0 & 0 & 0 \\ \lambda & \lambda & \beta & 0 & 0 & 0 \\ 0 & 0 & 0 & \mu & 0 & 0 \\ 0 & 0 & 0 & 0 & \mu & 0 \\ 0 & 0 & 0 & 0 & 0 & \mu \end{bmatrix} \begin{Bmatrix} \epsilon_{11} - \alpha \Delta T \\ \epsilon_{22} - \alpha \Delta T \\ \epsilon_{33} - \alpha \Delta T \\ 2\epsilon_{32} \\ 2\epsilon_{13} \\ 2\epsilon_{12} \end{Bmatrix} \quad (13)$$

where $\beta = 2\mu + \lambda$.

2.2. Software architecture

The software is divided in two main sets of code. The first one is a pre-processor module developed in MATLAB that can be used to fit a B-Spline curve to the measured volume fraction distribution using the least squares method. In addition, the pre-processor can also be used to compute the homogenized elastic properties according to the volume fraction distribution of the composite to be analyzed.

The second set is comprised of Fortran subroutines that are called by Abaqus during the analysis. The Fortran subroutines

are integrated into Abaqus as user-defined material (UMAT) for stress analysis and user-defined temperature field (UTEMP) for thermomechanical problems. The UMAT provide the material's constitutive behavior at the Gauss point level according to its geometrical coordinates. This way, any complex FGM structure subjected to thermal and/or mechanical loads can be analyzed.

The general flowchart of the analysis using MicroFEA 1.0 is shown in Fig. 1.

During the analysis, the chosen user-subroutine (UMAT) is called by Abaqus for each Gauss point of the finite element mesh at each increment or iteration, depending on the chosen solver. At each of these calls to the UMAT, the strain vector (STRAN), the temperature (TEMP), the material parameters, and the X, Y and Z coordinates (COORDS) of the point are passed on to the subroutine. These coordinates are used to evaluate the volume fraction at each Gauss point using a B-Spline (Eq. (4)) or a closed-form mathematical expression (e.g. Eq. (1)). The computed volume fraction and the phase properties are passed to the homogenization subroutines to evaluate the effective material properties. These properties are then used by the UMAT to calculate the constitutive matrix (DDSDDE) and the stress vector (STRESS) from the given strain vector, according to Eq. (13).

In addition to UMAT, the analysis of FGM structures subjected to thermomechanical loading requires the use of UTEMP subroutines to define the temperature field. Abaqus calls the chosen UTEMP to evaluate the temperature of each Gauss point and pass this temperature as argument to the UMAT.

2.3. Software functionalities

MicroFEA allows the definition of volume fraction variation using standard closed-form expressions (e.g. exponential and power-law) and B-Spline curves. The former is simpler for FGM design and parametric studies while the latter is more adequate to represent experimentally measured data and provides more flexibility to FGM optimization.

As aforementioned, MicroFEA utilizes the volume fraction profile as the input parameter for the homogenization. The use of the volume fraction distribution profile instead of the modulus profile is important because the measurement of the volume fraction distribution is more easily attained experimentally.

The B-Spline control points are evaluated by least squared fitting. By default, the software uses cubic splines and open knot vectors with equally spaced interior knots, but the user can change these parameters in order to obtain a better fitting. When the fitting process is finalized by the pre-processor, the knot vector \mathcal{E} and control points data (V_f) are available to be used as input data in the ABAQUS interface, as discussed in Section 2.4.

Fig. 2 shows the fitted B-Spline curve of a typical volume fraction profile of a Titanium aluminide (Al_3Ti) intermetallic composite produced by centrifugal casting. It can be seen that the B-Spline curve is capable of better accounting for the jaggedness of the actual volume fraction distribution comparatively to an exponential fit.

MicroFEA was developed for 3D thermomechanical analysis of FGM structures based on Eqs. (6)–(13). However, in most FGMs the volume fraction varies along one direction only, such as the thickness in plates and shells and the radius in pipes and pressure vessels. Therefore, univariate B-Splines are used to represent the volume fraction gradation along the chosen direction.

In addition to the standard usage described in Section 2.2, MicroFEA allows also an alternative approach where the effective properties are computed before the analysis using the chosen method and the properties of each phase. The values of the effective properties are then fitted using B-Splines. It is important to note that the standard approach is more general, since it can

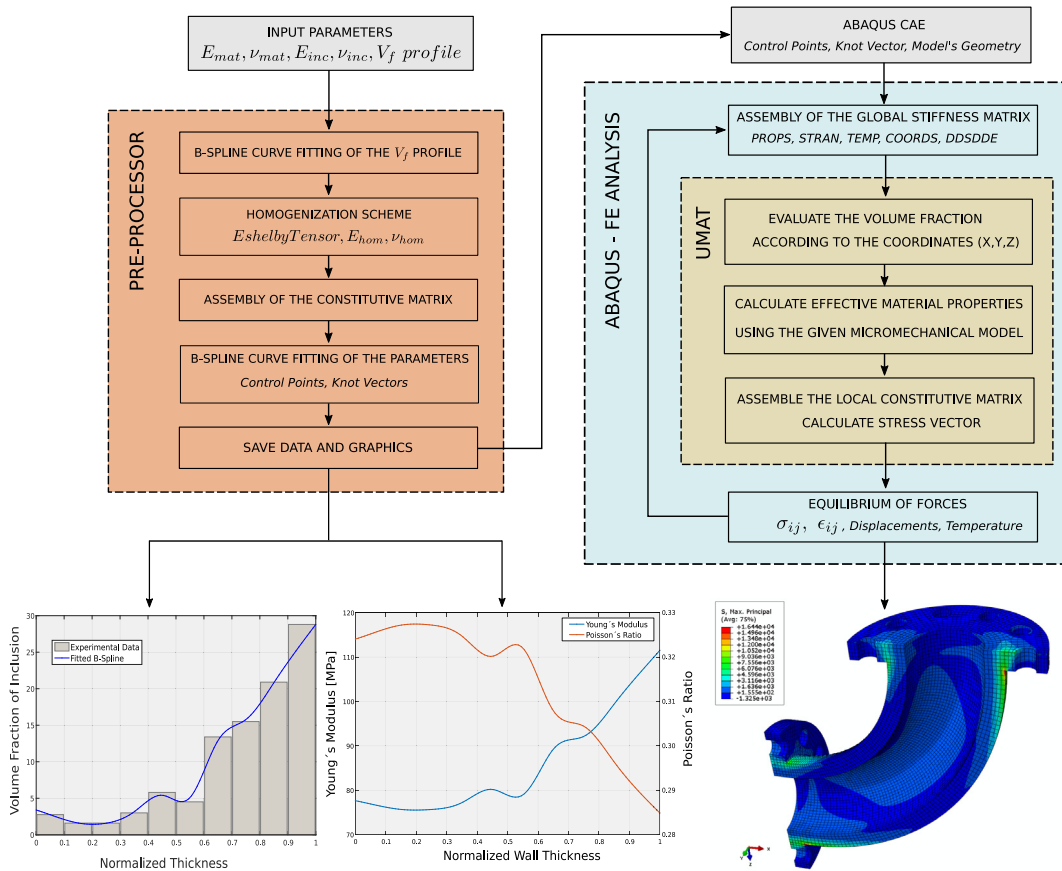


Fig. 1. MicroFEA 1.0 operation flowchart.

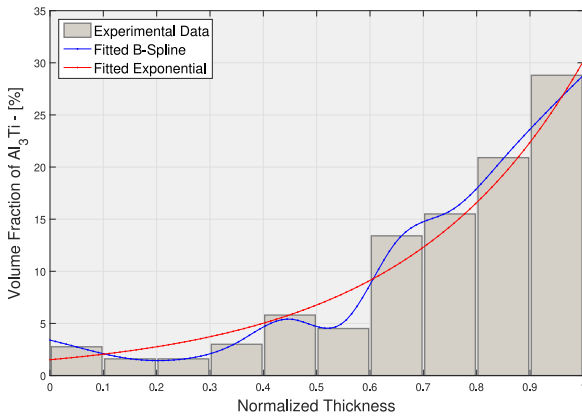


Fig. 2. Volume fraction profile (experimental data from [19]).

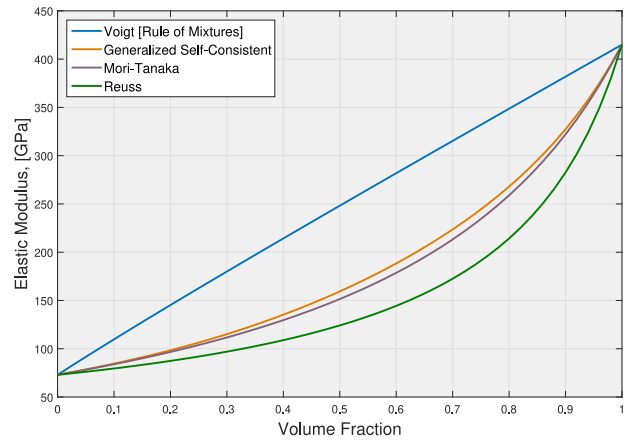


Fig. 3. Different homogenization methods.

be used for temperature-dependent properties and extended for nonlinear material models (e.g. elasto-plasticity). On the other hand, the alternative approach based on the use of fitted effective properties is more computationally efficient since it does not require the use of costly homogenization methods for each Gauss point, but can be used only for materially linear analysis with temperature independent properties.

The pre-processor has four homogenization schemes implemented in the current version: Voigt, Reuss, Mori-Tanaka, and Generalized Self-Consistent. This permits a parametric analysis among the different models for instance. An envelope analysis considering the Voigt and Reuss models as the lower and upper boundaries is also possible. The homogenized properties can also

be used in other environments where the FE Analysis is not the ultimate goal. Fig. 3 shows the modulus profiles for each of the homogenization schemes considering a volume fraction variation from 0 to 100%.

The UMAT is capable of working with finite element models containing homogeneous and FGM materials simultaneously. The user must only define which sections of the model should be assigned to one or the other. This gives the freedom to model FGM structures that interact with surrounding homogeneous counterparts.

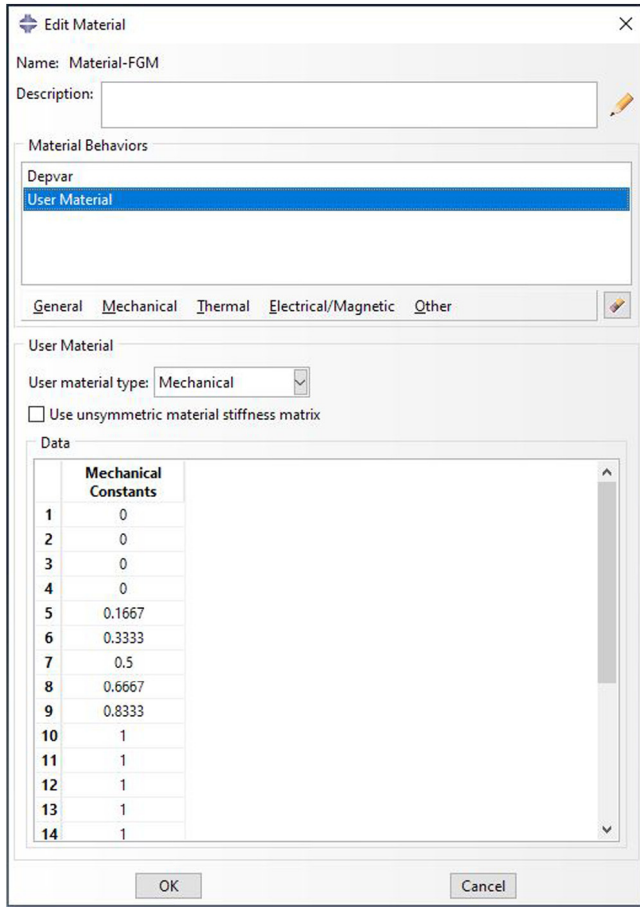


Fig. 4. Input parameters in Abaqus CAE material module.

2.4. Software use

The software is comprised of two main parts, the pre-processor and the Abaqus subroutines. The pre-processor is formed by a set of Matlab .m files that contain the four micromechanical models and the B-Spline curve fitting algorithms. These files can be invoked used as standalone functions to calculate the effective properties for a certain volume fraction or by other .m file to study the effect of micromechanical models and volume fraction variation (see the *DemoMicroFEA.m* file). The set of functions also allow the user to fit the B-Spline curve to a given dataset providing the knot vector and control points that are later used in Abaqus CAE.

The Abaqus subroutines can accept input data either from the material module in the CAE or directly from the Fortran subroutine. When the CAE is chosen, the properties are passed as the PROPS vector. Fig. 4 shows the input data that was obtained in the pre-processor analysis being entered in the material module. The user should input the 13 initial values corresponding to the knot vector values, the next 9 positions should be filled with the control points. Lastly, the N and P values ought to be entered respectively.

To run the analysis the user must specify the appropriate subroutine. Abaqus requires that the Fortran subroutines must be present in the same directory of the analysis, which is usually the *Temp* folder. In the *Job* module the user must select *Edit job* then select the *General* tab. The user subroutine is then selected and the job will be ready for analysis. (See Fig. 5.)

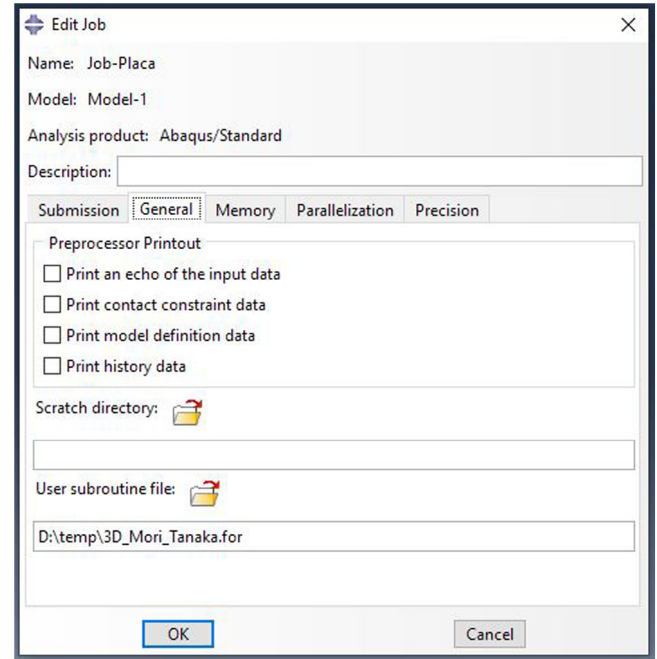


Fig. 5. Input parameters in Abaqus CAE material module.

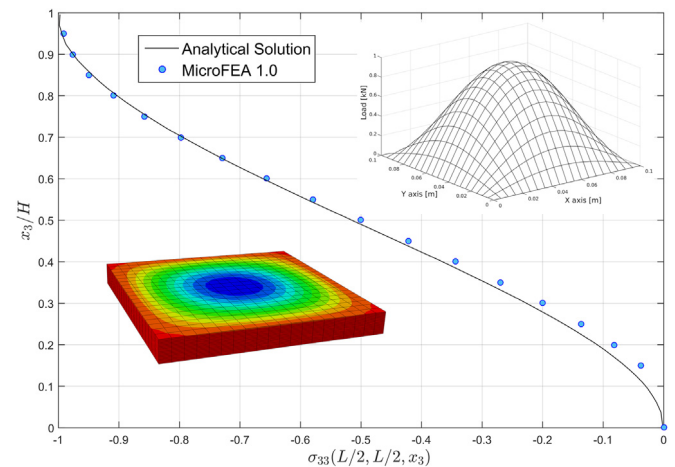


Fig. 6. Stress profile along the plate thickness (analytical solution found in [27]).

3. Examples

The first example corresponds to the analysis of a simply supported functionally graded square plate with $h/L = 1/10$ and subjected to a transverse load given by $q(x, y) = \sin(\pi x/L) \sin(\pi y/L)$, where L is the plate length. The analytical solution based on the asymptotic expansion method for three-dimensional analysis of inhomogeneous plates [27] was used to compare against the results provided by the MicroFEA analysis. All the necessary information regarding geometry, boundary conditions and material properties is provided in the reference paper and was not repeated here for sake of brevity. Fig. 6 shows a very good agreement between numerical and analytical normal stresses through the plate thickness.

A square plate with the same geometry and boundary conditions, but under an uniform transverse load (q_0) was used to compare the two most popular homogenization schemes (Mori-Tanaka and Voigt). The matrix is considered to be aluminum and

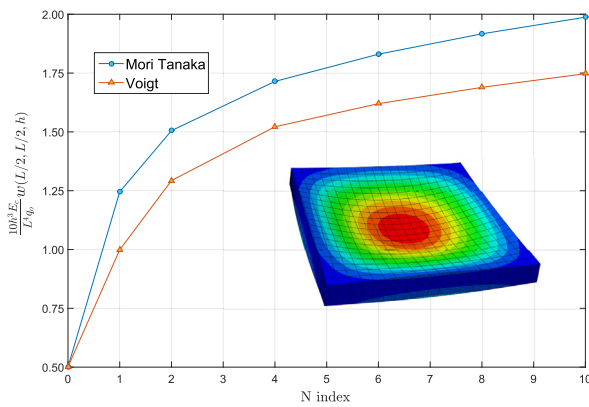


Fig. 7. Non-dimensional transverse deflection at the center of an FGM plate.

the ceramic inclusion is alumina (Al_2O_3), whose properties are; $E_{mat} = 70$ GPa, $\nu_{mat} = 0.3$, $E_{inc} = 380$ GPa, $\nu_{inc} = 0.3$. Fig. 7 presents the non-dimensional transverse deflection at the center of the plate for several power indexes N , showing a significant difference in results of the two micromechanical models, since the widely used Voigt approach overestimates the material stiffness leading to smaller displacements.

The next example is an FGM pipe joint made out of aluminum and Silicon Carbide (Al/SiC). The part is engineered to have a wear-resistant inner surface and also to minimize the thermal effects of the hot fluids circulating through it and prevent bursting from high temperature creep. This model was constrained at the two flanges and was subjected to temperatures of $100^\circ C$ on the inside of the tube and $20^\circ C$ on the outside. The volume fraction distribution of the inclusions along the pipe wall was assumed to vary in a similar way to the profile depicted in Fig. 2 but with the ceramic-rich side being the inner most surface and the ceramic depleted part corresponding to the outer surface. The X, Y and Z coordinates were used to create a normalized radius ranging from 0 to 1 going from the inner surface to its outer surface and following the curvature of the pipe bent. The trigonometric relationships can be found in the Fortran subroutine corresponding to this example. An internal pressure of 100 psi was also applied internally to the pipe. Fig. 8 presents the Von Mises stress field developed on the part. The material properties are; $E_{Al} = 70$ GPa, $\nu_{Al} = 0.33$, $E_{SiC} = 410$ GPa, $\nu_{SiC} = 0.18$. The results seen in Fig. 7 could be used for improvements in the engineering design of the part or to achieve the optimal distribution of the ceramic inclusions along the wall thickness for example.

4. Impact

The proposed software package represents an excellent tool for researchers and engineers to analyze complex FGM composite parts or structures. Currently, there are no software tools that are readily and freely available for the design and analysis of functionally graded composites.

The researchers working with FGMs and composites in general will be able to reuse the existing mean-field homogenization functions in other applications with different problem set-ups. In other words, practitioners will be able to employ these techniques in various applications, such as bio-medical implant development, vehicles and airplane parts and chemical processing plant parts.

The software package presented here can also be used to pursue new research questions in different areas such as topological optimization of composite structures, material optimization, and thermomechanical analysis of heterogeneous materials, to name

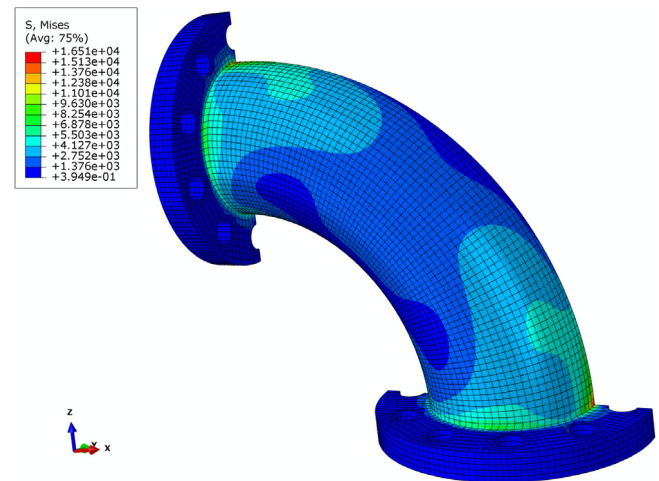


Fig. 8. FGM Pipe joint.

a few. Furthermore, we anticipate that the MATLAB functions and subroutines presented herein can be directly used by the industry to simulate and improve the quality of their FGM products.

5. Conclusions

Micro FEA 1.0, a software package to help in the design and analysis of Functionally Graded Materials (FGM) using the Finite Element Method, was presented in this paper. The software allows the definition of the volume fraction variation using of standard closed-form mathematical expressions or B-Splines curves. The former approach simplifies the analysis and design process while the latter increases the design flexibility for optimization purposes and allows the accurate representation of volume fraction profiles measured in laboratory.

The software also features mean-field micromechanics homogenization functions to evaluate the composite effective properties. The Abaqus user-material subroutines (UMATs) are designed to work with heterogeneous materials at the integration points level, and do not require custom-designed elements. The software is provided under the GNU General Public License and is expected to be a widely used framework for analysis, design and optimization of FGM structural components.

Acknowledgment

The authors gratefully acknowledge the financial support provided by CNPq (Conselho Nacional de Desenvolvimento Científico e Tecnológico), Brazil.

Declaration of competing interest

The authors declare that they have no known competing financial interests or personal relationships that could have appeared to influence the work reported in this paper.

References

- [1] Koizumi M. FGM activities in Japan. *Composites B* 1997;28(1–2):1–4. [http://dx.doi.org/10.1016/S1359-8368\(96\)00016-9](http://dx.doi.org/10.1016/S1359-8368(96)00016-9).
- [2] Shen H-S. *Functionally graded materials: nonlinear analysis of plates and shells*. CRC Press; 2009.
- [3] Gupta A, Talha M. Recent development in modeling and analysis of functionally graded materials and structures. *Prog Aerosp Sci* 2015;79:1–14. <http://dx.doi.org/10.1016/j.paerosci.2015.07.001>.

- [4] Xu C, Todd RI. Functionally graded ceramics by a new in situ processing route: residual stress and wear resistance. *J Eur Ceram Soc* 2015;35(9):2693–8. <http://dx.doi.org/10.1016/j.jeurceramsoc.2015.02.032>.
- [5] Ge W, Zhao C, Wang B. Thermal radiation and conduction in functionally graded thermal barrier coatings. Part I: Experimental study on radiative properties. *Int J Heat Mass Transfer* 2019;134:101–13. <http://dx.doi.org/10.1016/j.ijheatmasstransfer.2019.01.018>.
- [6] Bulatova R, Bahl C, Andersen K, Kuhn LT, Pryds N. Functionally graded ceramics fabricated with side-by-side tape casting for use in magnetic refrigeration. *Int J Appl Ceram Technol* 2014;12(4):891–8. <http://dx.doi.org/10.1111/ijac.12298>.
- [7] Chai H, Mielezko AJ, Chu SJ, Zhang Y. Using glass-graded zirconia to increase delamination growth resistance in porcelain/zirconia dental structures. *Dent Mater* 2018;34(1):e8–14. <http://dx.doi.org/10.1016/j.dental.2017.11.004>.
- [8] Kumar S, Reddy KM, Kumar A, Devi GR. Development and characterization of polymer–ceramic continuous fiber reinforced functionally graded composites for aerospace application. *Aerosp Sci Technol* 2013;26(1):185–91. <http://dx.doi.org/10.1016/j.ast.2012.04.002>.
- [9] Thivillon L, Bertrand P, Laget B, Smurov I. Potential of direct metal deposition technology for manufacturing thick functionally graded coatings and parts for reactors components. *J Nucl Mater* 2009;385(2):236–41. <http://dx.doi.org/10.1016/j.jnucmat.2008.11.023>.
- [10] Arsha A, Jayakumar E, Rajan T, Antony V, Pai B. Design and fabrication of functionally graded in-situ aluminium composites for automotive pistons. *Mater Des* 2015;88:1201–9. <http://dx.doi.org/10.1016/j.matdes.2015.09.099>.
- [11] Mahmoud D, Elbestawi M. Lattice structures and functionally graded materials applications in additive manufacturing of orthopedic implants: A review. *J Manuf Mater Process* 2017;1(2):13. <http://dx.doi.org/10.3390/jmmp1020013>.
- [12] Mao Y, Ai S, Fang D, Fu Y, Chen C. Elasto-plastic analysis of micro FGM beam basing on mechanism-based strain gradient plasticity theory. *Compos Struct* 2013;101:168–79. <http://dx.doi.org/10.1016/j.compstruct.2013.01.027>.
- [13] Seifi R. Stress intensity factors for internal surface cracks in autofrettaged functionally graded thick cylinders using weight function method. *Theor Appl Fract Mech* 2015;75:113–23. <http://dx.doi.org/10.1016/j.tafmec.2014.11.004>.
- [14] Rouhi S, Alavi SH. On the mechanical properties of functionally graded materials reinforced by carbon nanotubes. *Proc Inst Mech Eng C* 2017;232(9):1632–46. <http://dx.doi.org/10.1177/0954406217706096>.
- [15] Jrad H, Mars J, Wali M, Dammak F. Geometrically nonlinear analysis of elastoplastic behavior of functionally graded shells. *Eng Comput* 2018. <http://dx.doi.org/10.1007/s00366-018-0633-3>.
- [16] Martínez-Pañeda E. On the finite element implementation of functionally graded materials. *Materials* 2019;12(2):287. <http://dx.doi.org/10.3390/ma12020287>.
- [17] Do D, Lee D, Lee J. Material optimization of functionally graded plates using deep neural network and modified symbiotic organisms search for eigenvalue problems. *Composites B* 2019;159:300–26. <http://dx.doi.org/10.1016/j.compositesb.2018.09.087>.
- [18] Medeiros Jr. MS, Parente Jr. E, de Melo AMC. Influence of the micromechanics models and volume fraction distribution on the overall behavior of SiC/Al functionally graded pressurized cylinders. *Lat Am J Solids Struct* 2019;16(4). <http://dx.doi.org/10.1590/1679-78255433>.
- [19] Watanabe Y, Sequeira PD, Sato H, Inamura T, Hosoda H. Aluminum matrix texture in Al–Al₃Ti functionally graded materials analyzed by electron back-scattering diffraction. *Japan J Appl Phys* 2015;55(15):01AG03. <http://dx.doi.org/10.7567/jjap.55.01ag03>.
- [20] Watanabe Y, Zhou Q, Sato H, Fujii T, Inamura T. Microstructures of Al–Al₃Ti functionally graded materials fabricated by centrifugal solid-particle method and centrifugal in situ method. *Japan J Appl Phys* 2017;56(1S). <http://dx.doi.org/10.7567/jjap.56.01ag01>.
- [21] Piegł L, Tiller W. *The NURBS book*. Springer Berlin Heidelberg; 1995. <http://dx.doi.org/10.1007/978-3-642-97385-7>.
- [22] Arfken GB, Weber HJ, Harris FE. Green's functions. In: *Mathematical methods for physicists*. Elsevier; 2013, p. 447–67. <http://dx.doi.org/10.1016/b978-0-12-384654-9.00010-4>.
- [23] Hollister SJ, Kikuchi N. A comparison of homogenization and standard mechanics analyses for periodic porous composites. *Comput Mech* 1992;10(2):73–95. <http://dx.doi.org/10.1007/bf00369853>.
- [24] Benveniste Y. A new approach to the application of Mori-Tanaka's theory in composite materials. *Mech Mater* 1987;6(2):147–57. [http://dx.doi.org/10.1016/0167-6636\(87\)90005-6](http://dx.doi.org/10.1016/0167-6636(87)90005-6).
- [25] Aboudi J, Arnold S, Bednarczyk B. *Micromechanics of composite materials*. Oxford: Butterworth-Heinemann; 2013. <http://dx.doi.org/10.1016/B978-0-12-397035-0.05001-1>.
- [26] Turner P. Thermal-expansion stresses in reinforced plastics. *J Res Natl Bur Stand* 1946;37(4):239. <http://dx.doi.org/10.6028/jres.037.015>.
- [27] Reddy J, Cheng Z-Q. Three-dimensional thermomechanical deformations of functionally graded rectangular plates. *Eur J Mech A Solids* 2001;20(5):841–55. [http://dx.doi.org/10.1016/s0997-7538\(01\)01174-3](http://dx.doi.org/10.1016/s0997-7538(01)01174-3).